# Title: Evolution of Cajal-Retzius Cells in Vertebrates from an Ancient Class of Tp73+ Neurons

**Authors:** Elias Gumnit[1], Giacomo Gattoni[1], Jamie Woych[1], Astrid Deryckere[1#], Prabesh Bhattarai[2,3], J Andrew Gillis[4], Caghan Kizil[2,3], Maria Antonietta Tosches[1*]

**Affiliations:**
[1] Department of Biological Sciences, Columbia University, New York, NY, USA.
[2] Department of Neurology, Columbia University Irving Medical Center, New York, NY, USA
[3] The Taub Institute for Research on Alzheimer's Disease and the Aging Brain, Columbia University Irving Medical Center, New York, NY, USA
[4] Bay Paul Centre, Marine Biological Laboratory, Woods Hole, MA, USA

[#] Present address: Laboratory of Reproductive Genomics, KU Leuven, Leuven, Belgium

* Corresponding author. Email: mt3353@columbia.edu

**Abstract:** In the developing cerebral cortex, Cajal Retzius (CR) cells are early-born neurons that orchestrate the development of mammalian-specific cortical features. However, this cell type has not been conclusively identified in non-mammalian species. Here we studied neurons expressing *Tp73*, a transcription factor specifically expressed in most mammalian CR cells. Comparisons of chicken, salamander, zebrafish, and little skate data indicate that *Tp73*-expressing neurons have conserved spatial distribution and transcriptomic signatures in vertebrates. Among the conserved Tp73-expressing cell types we find CR cells and*Tp73*+ external tufted cells (ETCs) in the olfactory bulb of jawed vertebrates. ETCs and CR cells share the expression of most "canonical" CR cell transcription factors, such as *Tp73, Lhx1, Lhx5, Ebf3,* and *Nr2f2*, indicating that they are sister cell types. Our findings suggest that CR and ETCs evolved in stem vertebrates from cells involved in olfactory processing, with CR cells progressively acquiring new specialized roles in developmental signaling.

**Main Text:** The forebrain is the brain region that underwent the most dramatic changes in vertebrate evolution (*1*). In mammalian ancestors, the drastic expansion of the pallium (dorsal telencephalon) occurred with several innovations, including the anatomical and functional diversification of cortical regions, a six-layered neocortex, and a folded hippocampus. Changes in cortical development may underlie the evolution of these novelties (*1*, *2*). To investigate the underpinnings of these changes, we focused on Cajal-Retzius (CR) cells, a multifunctional cell type with critical roles in the development of mammalian-specific cortical traits (*3–6*). In mammals, CR cells are born in the ventral pallium, cortical hem, septum, and prethalamic eminence (PThE), and then migrate tangentially in the marginal zone to cover the entire telencephalic vesicle (*7–12*). These cells are the major source of Reelin, a secreted molecule that regulates the radial migration of immature neurons during corticogenesis (*13*, *14*). CR cells also control cortical arealization, serve as pioneer neurons in the hippocampus and olfactory system, influence hippocampal morphogenesis, and regulate circuit assembly in the hippocampus and neocortex (*8*, *14–21*).

Notably, while CR cells are the first neurons that develop in the mammalian pallium, their evolution remains highly debated. Markers of mammalian CR cells, including Reelin and the transcription factor p73, are expressed in scattered pallial cells in developing lizard, crocodile, chicken, frog, and fish brains (*22–26*). A recent study proposed that CR cells existed already in tetrapod ancestors (*26*), but the interpretation of chick data is contentious (*25*, *27*, *28*), and fishes remain poorly investigated. The expression of single CR markers remains insufficient to conclude whether CR cells exist in non-mammals: none of these markers are CR-specific, but it is only their *combined* expression that defines CR identity (*3*).

With the advent of single-cell RNA sequencing, mammalian CR cells have been well characterized at the transcriptomic level, and express a core set of transcription factors (TFs)

including: *Tp73, Tbr1, Lhx1, Lhx5, Ebf2, Ebf3, Nr2f2, Nhlh2,* and *Barhl2* (with *Tp73* and *Ebf3* missing in ventral-pallium derived cells) (*5, 29*). Among these, *Tp73* (*Trp73* in mice) encodes for p73 and is expressed in CR cells derived from medial sources (PThE, septum, and hem). (For simplicity, hereafter we refer to the mouse *Trp73* gene as *Tp73*). *Tp73* is a key player in the gene regulatory network that establishes medial CR identity: mutant mice display abnormal cortical lamination and hippocampal malformations in conjunction with loss of medial CR cells (*22, 25*).

Given its specificity and functional relevance, *Tp73* served as a logical entry point for our analysis of CR cell identity and distribution across vertebrate species. We found that *Tp73* defines a diverse and evolutionarily-conserved family of neurons, including CR cells, but also neurons in the olfactory bulb (OB) and in the ventral forebrain. Our comparison of multiple vertebrate species suggests that CR cells were already present in vertebrate ancestors and share evolutionary origins with a *Tp73*-expressing neuron type in the OB, raising new scenarios on the early evolution of this enigmatic cell type.

**Conserved populations of *Tp73*+ neurons in vertebrates**

In the developing mouse brain, *Tp73* is expressed in neurons distributed within the pallium, subpallium, olfactory bulb (OB), preoptic area (POA) and PThE (in the diencephalon), and also in some non-neuronal cells including the choroid plexus, which is hem-derived (Fig. 1A) (*30*). While pallial *Tp73*+ neurons are CR cells, many of the diencephalic *Tp73*+ neurons are believed not to be CR cells due to their lack of *Reln* expression (*31, 32*) (Fig. 1A).

Using HCR *in situ* hybridization, we characterized the distribution of *Tp73*+ neurons during brain development in multiple species representing the major vertebrate clades. Scattered *Tp73*+ neurons have been reported in the developing chick brain (*25*). These *Tp73*+ neurons are most dense near the cortical hem and grow sparser laterally into the medial and dorsal pallium (Fig. 1B). We also observed *Tp73*+ neurons in the chick subpallium, PThE, and OB (Fig. 1B,

fig. S1A). Overall, the distribution pattern was similar to the one previously observed in lizards embryos, where *Tp73*+ neurons were found in the PThE, subpallium, and OB, but with only sparse *Tp73*+ neurons in the pallium (*23*) (Fig. 1A). In the salamander *Pleurodeles waltl,* we found scattered *Tp73*+ neurons also distributed throughout the pallium - with higher density around the hem - from early (st.36) to late stages (st.50) of pallial neurogenesis (*33*). In addition, *Tp73*+ cells were visible in the OB, PThE, and subpallium (Fig. 1C, fig. S1B, video. S1).

We then extended our analysis to two distantly-related fish species, a teleost (zebrafish) and a cartilaginous fish (little skate *Leucoraja erinacea*). In the developing zebrafish forebrain, *tp73*+ cells were present in the same brain regions described in tetrapods, with sparse *tp73*+ neurons in the pallium (Fig. 1D, fig S1C, video. S2). In the developing skate, *Tp73*+ neurons were found in high density in the OB and pallium, and more sparsely in the subpallium and putative PThE, consistent with other vertebrates (Fig. 1E, fig. S1D).

In the adult mouse brain, *Tp73*+ neurons persist in the OB, basal forebrain, and pallium, although only a small percentage of CR cells in the pallium survives to adulthood (*34*). Consistently, we found *Tp73*+ neurons in the same brain areas, plus the PThE, in adult salamander, zebrafish, little skate, and in the bichir fish *Polypterus senegalus* (a non-teleost ray-finned fish), but with a drastic reduction of the density of *Tp73*+ pallial cells, particularly in skates (fig. S2, video. S3-4). These results suggest that the pattern of *Tp73* expression is conserved across jawed vertebrates, with at least some *Tp73* neurons in the developing pallium, the region in mammals where *Tp73* is highly specific to CR cells.

Next, we asked whether non-mammalian *Tp73*+ neurons are similar to mammalian CR cells at the transcriptome level. For this we relied on our recent high quality scRNA-seq dataset of the developing salamander brain (*35*), which spans eight developmental stages and multiple brain regions. We found that TFs usually associated with CR cells - *Tp73*, *Lhx1*, *Lhx5*, *Nr2f2*,

*Ebf2*, *Ebf3*, and *Barhl2* - were expressed in one heterogeneous cluster of salamander cells (Fig. 2A-B, fig. S3A). Furthermore, this cluster expressed neuronal markers such as *Snap25*, and glutamatergic markers such as *Slc17a6*, which clearly differentiated it from other non-neuronal *Tp73*+ cells (fig. S3B). To further determine whether these salamander *Tp73*+ neurons are transcriptomically similar to mouse CR cells, we compared our scRNAseq data with a developmental mouse brain dataset (*36*), restricting our analysis to mature neurons (see Methods). We used two independent methods to compare the salamander and mouse datasets. First, we computed the gene specificity index (GSI) correlation (*37*) of all neuron classes in salamander and mouse, and found that the salamander *Tp73*+ neurons are most similar to mouse CR cells (Fig. 2C). Second, using manifold integration (*38*) for the joint analysis of the two data sets, we identified an integrated cluster that includes salamander *Tp73*+ neurons and mouse CR cells, supporting the transcriptomic similarity of these cell types (Fig. 2D, fig. S4A-D). These data suggest a close transcriptomic similarity of salamander *Tp73*+ neurons and mouse CR cells.

Next, we compared transcriptomic data from salamander and zebrafish to assess the similarity of their *Tp73*+ neurons. In a dataset by Pandey et al. (*39*) from the developing zebrafish forebrain, a glutamatergic cell type annotated as "OB" expressed many of the TFs characterizing mammalian CR cells such as *lhx1a*, *lhx5*, *ebf3*, and *barhl2* (Fig. 2E-F, fig. S5A-F); *tp73* was poorly detected in this dataset, probably due to technical reasons; however, this gene was detected in a more deeply-sequenced adult dataset (*40*), where it was coexpressed with other CR TFs (see fig. S5L-S). GSI correlation analysis of zebrafish and salamander neurons showed a significant correlation between salamander *Tp73*+ neurons and the zebrafish "OB" cluster; markers of OB mitral cells were instead expressed in a separate set of cells (Fig. 2G, fig. S5H-K). In addition, integration of salamander and zebrafish data showed co-clustering of zebrafish "OB" cells and a subset of salamander *Tp73*+ neurons; a second group of salamander

*Tp73*+ neurons co-clustered with zebrafish diencephalic neurons, suggesting transcriptomic heterogeneity (Fig. 2H, fig. S4E-H). These results show that *Tp73*+ neurons are overall highly similar at the transcriptomic level in mouse, salamander, and zebrafish, supporting their evolutionary conservation in vertebrates.

**Heterogeneity of salamander *Tp73*+ neurons**

Next, we sought to further characterize the heterogeneity of salamander *Tp73*+ neurons, to clarify their relationships with mammalian CR cells. To increase the power of our analyses, we merged *Tp73*+ clusters from larval and adult (*41*) scRNA-seq datasets, after noticing that *Tp73*+ neurons have conserved transcriptomes and spatial distribution across the salamander lifespan (fig. S2A-B). This salamander *Tp73*+ dataset, restricted to neurons, contained 982 cells (Fig. 3A, fig. S6).

After clustering and differential gene expression analysis, we identified three major classes of *Tp73*+ neurons, each including multiple clusters. The first class comprised late progenitors and immature neurons, as indicated by the expression of the proliferation marker *Mki67*, low levels of the synaptic gene *Snap25*, and markers of immature neurons like *Vim* and *Neurod4* (clusters im1-2, Fig. 3A-B). These clusters were uniquely labeled by *Gmnc* and *Cccno*, members of a multiciliation gene module expressed transiently during CR differentiation in mice (*25*). Double HCR *in situ* hybridization for *Gmnc* and *Ccno* showed coexpression with *Tp73* in sparse cells in the hem, septum, and PThE (fig. S7). These observations suggest that clusters im1-2 are cells in the process of acquiring a terminal *Tp73*+ neuronal fate.

The other two classes we identified as mature *Tp73*+ neurons. The first class (clusters m1.1 to 1.4) shared some of the defining features of CR cells, including *Ebf2* and *Ebf3* expression and absence of *Foxg1* expression. The second class (clusters m2.1 to m2.8) expressed the unique combination of *Stk32a*, *Elfn1*, and *Sorcs1* (Fig. 3B). We performed HCRs to locate

these two distinct populations in the developing brain. *Stk32a* and *Tp73* (m2 class) were coexpressed in the subpallium and PThE, but not in the OB or pallium. In contrast, *Ebf3* and *Tp73* (m1 class) were coexpressed in cells in the OB and pallium, but not in the subpallium or PThE (Fig. 3C, fig. S8A-B). We conclude that mature salamander *Tp73*+ neurons belong to spatially and molecularly distinct populations: a population of *Tp73*+ *Ebf3*+ neurons enriched in the anterior and dorsal forebrain, and a second population of *Tp73*+ *Ebf3*- neurons in the posterior and ventral forebrain. These two neuronal classes co-cluster with different sets of neurons in the zebrafish dataset, suggesting an ancient origin (fig. S8C).

Next, we explored further the heterogeneity of *Tp73*+ *Ebf3*+ neurons. Cluster m1.1 expressed high levels of *Nfix* and *Nfia*, markers of mammalian hem-derived CR cells (*29*). When staining for *Nfix*, we found coexpression with *Tp73* only in the pallium, including the hem region, and not in the OB (Fig. 3D, fig S8D-E). Conversely, clusters m1.2-4 expressed *Asic4* and *Cdhr1*, markers of mammalian OB glutamatergic neurons (*42*, *43*). *Asic4* showed the opposite pattern as *Nfix*, as it was coexpressed with *Tp73* in OB but not in pallium (Fig. 3D, fig S8D). This suggests that the *Tp73*+ *Ebf3*+ class of salamander neurons includes a pallial population with additional markers of mammalian CR identity, and an OB population expressing markers of OB glutamatergic neurons.

**Cajal-Retzius and olfactory bulb *Tp73*+ external tufted cells are sister cell types**

Next, we investigated whether the molecular and spatial heterogeneity of salamander *Tp73*+ neurons has counterparts in mammals. We isolated mouse *Tp73*+ neurons from the Allen Brain Cell (ABC) atlas (*34*) and compared them to the salamander *Tp73*+ neuron dataset. The ABC atlas, comprising the entire adult mouse brain, was chosen for its high sequencing depth, completeness, and matching MERFISH data, necessary to resolve subtle differences between

*Tp73*+ neurons types. This atlas includes 3 populations of *Tp73*+ neurons (Fig. 4A and fig. S9A-B). One is composed of subclass 118 ADP-MPO Trp73 and cluster 2111 LHA Barhl2 Glut_2, spatially located in the basal forebrain, specifically in areas annotated as the lateral hypothalamus and medial POA. A second group is the subclass 036 HPF CR Glut, which includes CR cells sampled from the adult cortex and hippocampus (Fig. 4A, fig. S9A). Finally, a third group is the supertype 0132 OB Eomes Ms4a15 Glut_3, which expresses *Lhx1* and *Ebf3* and corresponds to one type of external tufted cells (ETCs) (cluster ET2 in (*42*)). ETCs are a heterogeneous class of glutamatergic neurons in the mammalian OB; these cells, or at least a subset of them, are believed to be born in the pallium before migrating to the bulb (*44–46*). The *Tp73*+ ETCs have a characteristic spatial distribution: they surround the olfactory glomeruli (*42*), where they synapse with olfactory sensory neurons and other periglomerular interneurons (fig. S10). Using cross-species data integration, we found that classes of salamander *Tp73*+ neurons integrate with distinct mouse *Tp73*+ neurons. Salamander *Tp73*+ *Ebf3*- neurons co-clustered with mouse basal forebrain *Tp73*+ neurons, while salamander *Tp73*+ *Ebf3*+ neurons co-clustered with both CR and ETC cells in mice (Fig. 4B-E). Specifically, among salamander differentiated *Tp73*+ neurons, cluster m1.1 (*Nfix*+) co-clustered primarily with mouse CR cells, while clusters m1.3-4 (*Asic4*+) with mouse ETCs. GSI correlation analysis showed a similar trend, although this analysis was less sensitive than integration at distinguishing CR and ETC cells due to the high transcriptomic similarity between these two cell types (Fig. 4F). These comparisons indicate that salamander *Tp73*+ *Ebf3*+ *Nfix*+ neurons are homologous to mammalian CR cells, while salamander *Tp73*+ *Ebf3*+ *Asic4*+ neurons are homologous to ETCs.

Next, we wondered whether transcriptomically distinct CR and ETC cells exist in other vertebrate species. The available chicken (*47*) and zebrafish (*39*) datasets had several limitations, including low numbers of *Tp73*+ neurons, absence of OB sampling (in chicken), and relatively

lower sequencing depth (in zebrafish). Nevertheless, comparisons of chicken and zebrafish *Tp73*+ neurons with mouse ABC Atlas *Tp73*+ neurons supported the conclusion that the chicken *Tp73*+ neurons in (*47*) are CR cells (fig. S10, fig. S11A-C), and that most zebrafish *tp73*+ neurons in (*39*) are ETCs (fig. S11D-F). The fact that a few zebrafish cells co-clustered with mouse CR cells (fig. S11D-F), together with our tissue staining data (Fig. 1), is consistent with the possibility that CR cells also exist in teleosts.

To further support the existence of *Tp73*+ ETCs across vertebrates, we analyzed *Tp73* expression in the mature OB, where glomeruli are well defined. We observed *Tp73*+ neurons in the glomerular layer of salamander, bichir, zebrafish, and skate (Fig. 4G). In the three fish species, *Tp73* neurons were arranged in characteristic rings around the glomeruli (Fig. 4G). These results indicate that *Tp73*+ ETCs are a conserved neuron type in jawed vertebrates.

Finally, we asked whether the molecular identities of ETC and CR cells are defined by the expression of different sets of TFs, *i.e.* if they are genetically individuated (*48*). A comparison of TFs expressed in mouse CR and ETC cells but not in other OB glutamatergic neurons (see Methods) showed that mouse CR and ETC cells expressed different sets of TFs overall, but shared the expression of many TFs usually associated to CR identity (fig. S9D). Of these, *Nr2f2*, *Tp73*, *Dach1*, *Ebf3*, *Zeb2*, *Lhx1*, *Nr2f1*, *Tbr1*, *Id4* and *Hivep1* were expressed also in chicken CR cells and in salamander CR and ETCs (zebrafish ETCs lacked *Nr2f2*, *Tp73*, *Zeb2* and *Hivep1* expression, but we cannot rule out technical limitations) (Fig. 4H). Next, we wondered whether there were any TFs that could discriminate between ETC and CR cell identities across vertebrates. We identified the TFs that had conserved differential expression between ETC and CR cells in both salamander and mouse, and then assessed their expression in chicken CRs and zebrafish ETCs (see Methods). While we couldn't find any conserved ETC-specific TFs, we observed that *Zic1*, *Zic2*, and NFI TFs were expressed in CR but not in ETCs in

mouse and salamander, and that these TFs were expressed in chicken CRs too but not in zebrafish ETCs (Fig. 4I). Notably, in mouse this combination of TFs is enriched in hem-derived CR cells, suggesting that the CR cells sampled in salamander and chicken are mostly hem-derived, in line with our HCR data. The high degree of transcriptome and TF expression similarity of ETC and CR cells suggests that these cell types have a shared evolutionary origin, and that CR cells became further specialized by activating a CR-specific set of TFs.

**Transcriptomic divergence of vertebrate Cajal-Retzius cells**

The presence of CR cells in non-mammals challenges the notion that mammalian-specific cortical traits emerged with the appearance of this cell type in evolution. Alternatively, CR cells might be a conserved cell type with diverging characteristics across species.

Since a key effector of mammalian CR function is the secreted protein Reln, we first asked whether the coexpression of *Tp73* and *Reln* is conserved across vertebrate species. In the developing chick brain, we found robust overlap of *Tp73* and *Reln* in the pallium and hem, corroborating scRNA-seq data (Fig. 5A, fig. S6H). However, stainings for *Tp73* and *Reln* in salamander revealed coexpression only in rare *Tp73* pallial neurons, consistent with scRNA-seq (fig. S7H). Furthermore, there was no coexpression of *Tp73* and *Reln* in the pallium of developing skates and zebrafish. This is most striking in the developing skate brain, where *Reln* is clearly absent from the dense layer of *Tp73* neurons at the pallial surface (Fig. 5A, fig. S12). This suggests that strong coexpression of *Tp73* and *Reln* may be an amniote innovation, in line with observations in other species (*24*), and that *Reln* is not a conserved marker of CR cells across all vertebrates.

To identify other species-specific specializations, we searched genes with conserved and species-enriched expression in salamander and mouse CR cells. We computed in each species the differentially expressed genes between CR cells and other glutamatergic neurons in the

developing pallium (developing mouse data from (*25, 29*)); salamander CR cells were defined here as the mature neurons that integrate with mouse CR cells (Fig. 4) and ETCs were excluded (see Methods). As expected, the top shared markers included *Tp73*, *Ebf3, Zic1, Zic2* and other TFs (Fig. 5B). In addition, we found that the glutamate transporter *Slc17a6* (*Vglut2*), the glutamate receptor *Grm2*, and general markers of immature neurons (*Msi1*, *Sox9*, *Vim*) in CR cells from both species. *Cxcr4* and *Zic2*, essential for the proper migration and positioning of CR cells in mice (*49, 50*), were also expressed in salamander CR cells, suggesting the evolutionary conservation of molecular mechanisms of CR migration. The Netrin receptor *Unc5b* was also expressed in both salamander and mouse CR cells. Importantly, *Nectin-1* (encoded by *Pvrl1*), *N-cadherin* (*Cdh2*) and *Mllt4* (*Afdn*) were also expressed in CR from both species (fig. S13); in mouse, these adhesion molecules are crucial for the interaction between CR cells and cortical neurons during radial migration (*51*).

Interestingly, salamander and mouse CR cells expressed different sets of synaptic genes, with *Lgi2, Erbb4, Rpha3, Zdhhc22*, and *St8s1a4* enriched in salamander, and *Cacna2d2*, *Baiap2*, *S100a10*, and *Cpne2* enriched in mouse (Fig. 5B). This divergent use of synaptogenesis genes may be due to differences in wiring specificity, genetic drift, or some other species-specific adaptation. Furthermore, salamander and mouse CR cells differed in the expression of neurotrophic, cell cycle, and apoptotic genes, with *Ngfr*, *Serpinf1*, and *Erbb4* enriched in salamander, and *Cdkna1a* (p21), *Phlda3*, and *Tnfaip8* enriched in mouse (Fig. 5B), suggesting diverging mechanisms for the regulation of neuronal survival. Notably, the transcription factor *Dmrta2* was expressed in mouse but not salamander CR cells (see also Fig. 4G). *Dmrta2* knock-out mice have significantly reduced CR abundance (*52*), suggesting that gain of *Dmrta2* expression in amniote CR cells may have contributed to their higher number and density.

Finally, we reasoned that if CR cells have some role during pallial development also in non-mammals, their density should be highest during neurogenesis. This is clearly the case in the little skate (compare Fig. 1E and fig. S2). After counting *Tp73*+ neurons in the salamander medial and dorsal pallium, which are mostly CR cells, we saw that their density peaks during early pallial neurogenesis (*33, 35*) (stage 46, with ~9000 cells per mm^3), and gradually decreases later (Fig. 5C). Taken together, our data indicate that non-mammalian CR cells may be involved in early pallial development, but use a divergent set of molecular effectors including Reln.

**Discussion**

Our results demonstrate that there are two conserved classes of *Tp73*+ neurons in vertebrates, with distinct transcriptomes and spatial distribution. A first class (*Tp73*+ *Ebf3*- cells) comprises cells in the PThE and basal forebrain. The PThE is the developmental source of several types of glutamatergic neurons that then migrate to other brain regions, including the basal forebrain (*9, 53, 54*). We suggest that the *Tp73*+ *Ebf3*- cells we identified in salamander and zebrafish include the PThE and its basal forebrain derivatives. A second conserved class of *Tp73*+ *Ebf3*+ neurons includes cells located in the olfactory bulb and in the pallium, particularly in the hem region. Our transcriptomic analyses indicate that these cells belong to two distinct types, the *Tp73*+ external tufted cells and the *Tp73*+ Cajal-Retzius cells. Our results establish that CR cells existed at least in the last common ancestor of jawed vertebrates, in line with a recent scRNAseq study reporting CR cells in the shark *Scyliorhinus canicula* (*55*).

Interestingly, all the CR cells we identified in non-mammalian species express markers of mammalian hem-derived CR cells. Although the hem seems to be the most prominent source of CR cells outside mammals, it is possible that septum and PThE-derived CR cells also exist in

non-mammals, as suggested by *Tp73* expression in chicken and salamander (Fig. 1B-C) and *Ccno* and *Gmnc* expression in salamander (fig. S7). The evolution of ventral-pallium derived CR cells, which do not express *Tp73*, remains unresolved.

The non-mammalian CR cells show their highest density in the developing brain, suggesting they may play some role in pallial development like their mammalian counterparts. What exactly this ancestral CR function might be remains a matter of speculation. Here we find that *Reln* expression is not a conserved feature of vertebrate CR cells. This suggests that, if CR cells have a conserved function in all vertebrates, this function is Reln-independent. The marked increased expression of *Reln* in mammalian CR cells may thus relate to the emergence of mammalian-specific cortical features, such as radial migration and inside-out corticogenesis (*1*, *6*). Indeed, *Reln* deletion in mouse *Tp73*+ CR cells affects cortical lamination, but does not recapitulate the other defects caused by CR cells genetic ablation (*20*, *56*). Therefore, the regulation of radial migration by CR-derived Reln may have evolved with the transition from outside-in to inside-out corticogenesis, an innovation that took place in mammalian ancestors (*35*).

Besides regulating radial migration, mammalian CR cells have prominent roles in the assembly and maturation of neural circuits in the hippocampus (*15*, *21*, *57*, *58*) and neocortex (*59*). In neocortical layer 1, CR cells are part of large networks of spontaneously-active neurons (*60*), and regulate the spatial distribution of superficial layer interneurons and dendritic maturation in pyramidal neurons (*8*). In mammals, amphibians, non-avian reptiles, and certain fish species, the superficial neuropil layer (layer 1 in mammals) is a conserved site of integration of long-range inputs from cortical and subcortical areas, including sensory inputs relayed by thalamus (*41*, *61*). Thus, the modulation of circuit assembly might have been an ancestral function of CR cells (*17*, *62*). Intriguingly, spontaneous activity of the thalamus regulates CR

density in mouse layer 1 (*17*). It is tempting to speculate that the density of CR cells coevolved with the presence of sensory thalamic projections to the pallium, which are scarce in amphibians and possibly more abundant in cartilagineous fishes (*63*), where CR cells are particularly numerous during development.

Finally, our results reveal a surprising degree of transcriptomic similarity between CR cells and OB *Tp73*+ ETCs. Several observations suggest that CR cells and ETCs are sister cell types, evolved from an ancestral cell type present in the last common ancestor of vertebrates (or earlier) (Fig. 5D). First, in mouse and salamander these two cell types share the expression of a long list of TFs previously thought to be CR-specific, indicating that their transcriptomic similarity is not a result of convergent evolution. Second, lineage tracing experiments in mice indicate that some ETCs are born from pallial progenitors and then migrate to the OB, suggesting a shared developmental origin of CR and ETC cells (*45*, *46*). Third, CR and ETCs have similar electrophysiological properties: they receive strong inputs from GABAergic interneurons, display synchronous bursting, have prominent inward rectifying currents, and are connected by gap junctions (*4*, *64–68*). Fourth, both cell types have strong connections with the olfactory system: ETCs are directly postsynaptic to olfactory sensory neurons, whereas CR cells in the lateral olfactory tract, which function as guidepost neurons during development, might be among the lateral olfactory tract cells that receive second-order olfactory inputs from the bulb (*69*). We thus propose that CR and ETCs may have evolved by duplication and divergence from cells involved in early olfactory processing in vertebrate ancestors. As suggested by our TFs analysis, CR cells may have evolved by neofunctionalization and taken on new signaling functions to regulate circuit assembly in an expanded telencephalon (*70*) (Fig. 5D). Taken together, our findings highlight the complex relationships between molecular and functional cell type

evolution (*48*), and further support the hypothesis that olfactory circuits in ancestral vertebrates served as a developmental and functional blueprint for the evolving telencephalon.

**References and Notes**


1. F. García-Moreno, Z. Molnár, Variations of telencephalic development that paved the way for neocortical evolution. *Prog. Neurobiol.* **194**, 101865 (2020).

2. A. M. Goffinet, The evolution of cortical development: the synapsid-diapsid divergence. *Development* **144**, 4061–4077 (2017).

3. V. Elorriaga, A. Pierani, F. Causeret, Cajal-retzius cells: Recent advances in identity and function. *Curr. Opin. Neurobiol.* **79**, 102686 (2023).

4. S. Kirischuk, H. J. Luhmann, W. Kilb, Cajal-Retzius cells: update on structural and functional properties of these mystic neurons that bridged the 20th century. *Neuroscience* **275**, 33–46 (2014).

5. F. Causeret, M. X. Moreau, A. Pierani, O. Blanquie, The multiple facets of Cajal-Retzius neurons. *Development* **148**, dev199409 (2021).

6. M. Marín-Padilla, Cajal–Retzius cells and the development of the neocortex. *Copyright* © **21** (1998).

7. F. García-Moreno, L. López-Mascaraque, J. A. De Carlos, Origins and migratory routes of murine Cajal-Retzius cells. *J. Comp. Neurol.* **500**, 419–432 (2007).

8. C. A. de Frutos, G. Bouvier, Y. Arai, M. S. Thion, L. Lokmane, M. Keita, M. Garcia-Dominguez, P. Charnay, T. Hirata, D. Riethmacher, E. A. Grove, F. Tissir, M. Casado, A. Pierani, S. Garel, Reallocation of Olfactory Cajal-Retzius Cells Shapes Neocortex Architecture. *Neuron* **92**, 435–448 (2016).

9. N. Ruiz-Reig, B. Andrés, D. Huilgol, E. A. Grove, F. Tissir, S. Tole, T. Theil, E. Herrera, A. Fairén, Lateral Thalamic Eminence: A Novel Origin for mGluR1/Lot Cells. *Cereb. Cortex* **27**, 2841–2856 (2017).

10. F. Bielle, A. Griveau, N. Narboux-Nême, S. Vigneau, M. Sigrist, S. Arber, M. Wassef, A. Pierani, Multiple origins of Cajal-Retzius cells at the borders of the developing pallium. *Nat. Neurosci.* **8**, 1002–1012 (2005).

11. K. Takiguchi-Hayashi, M. Sekiguchi, S. Ashigaki, M. Takamatsu, H. Hasegawa, R. Suzuki-Migishima, M. Yokoyama, S. Nakanishi, Y. Tanabe, Generation of reelin-positive marginal zone cells from the caudomedial wall of telencephalic vesicles. *J. Neurosci.* **24**, 2286–2295 (2004).

12. G. Meyer, C. G. Perez-Garcia, H. Abraham, D. Caput, Expression of p73 and Reelin in the developing human cortex. *J. Neurosci.* **22**, 4973–4986 (2002).

13. G. D'Arcangelo, G. G. Miao, S. C. Chen, H. D. Soares, J. I. Morgan, T. Curran, A protein related to extracellular matrix proteins deleted in the mouse mutant reeler. *Nature* **374**, 719–723 (1995).

14. M. Ogawa, T. Miyata, K. Nakajima, K. Yagyu, M. Seike, K. Ikenaka, H. Yamamoto, K. Mikoshiba, The reeler gene-associated antigen on Cajal-Retzius neurons is a crucial molecule for laminar organization of cortical neurons. *Neuron* **14**, 899–912 (1995).

15. J. A. Del Río, B. Heimrich, V. Borrell, E. Förster, A. Drakew, S. Alcántara, K. Nakajima, T. Miyata, M. Ogawa, K. Mikoshiba, P. Derer, M. Frotscher, E. Soriano, A role for Cajal-Retzius cells and reelin in the development of hippocampal connections. *Nature* **385**, 70–74 (1997).

16. H. Supèr, A. Martínez, J. A. Del Río, E. Soriano, Involvement of distinct pioneer neurons in the formation of layer-specific connections in the hippocampus. *J. Neurosci.* **18**, 4616–4626 (1998).

17. I. Genescu, M. Aníbal-Martínez, V. Kouskoff, N. Chenouard, C. Mailhes-Hamon, H. Cartonnet, L. Lokmane, F. M. Rijli, G. López-Bendito, F. Gambino, S. Garel, Dynamic interplay between thalamic activity and Cajal-Retzius cells regulates the wiring of cortical layer 1. *Cell Rep.* **39**, 110667 (2022).

18. M. Barber, Y. Arai, Y. Morishita, L. Vigier, F. Causeret, U. Borello, F. Ledonne, E. Coppola, V. Contremoulins, F. W. Pfrieger, F. Tissir, S. Govindan, D. Jabaudon, V. Proux-Gillardeaux, T. Galli, A. Pierani, Migration speed of Cajal-Retzius cells modulated by vesicular trafficking controls the size of higher-order cortical areas. *Curr. Biol.* **25**, 2466–2478 (2015).

19. S. Alcántara, E. Pozas, C. F. Ibañez, E. Soriano, BDNF-modulated spatial organization of Cajal-Retzius and GABAergic neurons in the marginal zone plays a role in the development of cortical organization. *Cereb. Cortex* **16**, 487–499 (2006).

20. V. Elorriaga, B. Bouloudi, Y. Saillour, J. S. Morel, E. Delberghe, P. Azzam, M. X. Moreau, R. Stottmann, N. Bahi-Buisson, A. Pierani, N. Spassky, F. Causeret, Differential contribution of P73+ Cajal-Retzius cells and Reelin to cortical morphogenesis, *bioRxiv* (2024). https://doi.org/10.1101/2024.10.15.618167.

21. I. L. Glærum, K. Dunville, K. Moan, M. Krause, N. P. Montaldo, H. Kirikae, M. J. Nigro, P. Sætrom, B. van Loon, G. Quattrocolo, Postnatal persistence of hippocampal Cajal-Retzius cells has a crucial role in the establishment of the hippocampal circuit. *Development* **151**, dev202236 (2024).

22. G. Meyer, A. C. Socorro, C. G. P. Garcia, L. M. Millan, N. Walker, D. Caput, Developmental Roles of p73 in Cajal-Retzius Cells and Cortical Patterning. *J. Neurosci.* **24**, 9878–9887 (2004).

23. A. Cabrera-Socorro, N. C. Hernandez-Acosta, M. Gonzalez-Gomez, G. Meyer, Comparative aspects of p73 and Reelin expression in Cajal-Retzius cells and the cortical hem in lizard, mouse and human. *Brain Res.* **1132**, 59–70 (2007).

24. F. Tissir, C. Lambert De Rouvroit, J.-Y. Sire, G. Meyer, A. M. Goffinet, Reelin expression during embryonic brain development in Crocodylus niloticus. *J. Comp. Neurol.* **457**, 250–262 (2003).

25. M. X. Moreau, Y. Saillour, V. Elorriaga, B. Bouloudi, E. Delberghe, T. Deutsch Guerrero, A. Ochandorena-Saa, L. Maeso-Alonso, M. M. Marques, M. C. Marin, N. Spassky, A. Pierani, F. Causeret, Repurposing of the multiciliation gene regulatory network in fate specification of Cajal-Retzius neurons. *Dev. Cell* **58**, 1365–1382.e6 (2023).

26. S. Jiménez, N. Moreno, Analysis of the expression pattern of Cajal-Retzius cell markers in the Xenopus laevis forebrain. *Brain Behav. Evol.* **96**, 263–282 (2022).

27. T. Nomura, M. Takahashi, Y. Hara, N. Osumi, Patterns of neurogenesis and amplitude of Reelin expression are essential for making a mammalian-type cortex. *PLoS One* **3**, e1454 (2008).

28. F. García-Moreno, E. Anderton, M. Jankowska, J. Begbie, J. M. Encinas, M. Irimia, Z. Molnár, Absence of tangentially migrating glutamatergic neurons in the developing avian brain. *Cell Rep.* **22**, 96–109 (2018).

29. M. X. Moreau, Y. Saillour, A. W. Cwetsch, A. Pierani, F. Causeret, Single-cell transcriptomics of the early developing mouse cerebral cortex disentangle the spatial and temporal components of neuronal fate acquisition. *Development* **148** (2021).

30. A. Yang, N. Walker, R. Bronson, M. Kaghad, M. Oosterwegel, J. Bonnin, C. Vagner, H. Bonnet, P. Dikkes, A. Sharpe, F. McKeon, D. Caput, P73-deficient mice have neurological, pheromonal and inflammatory defects but lack spontaneous tumours. *Nature* **404**, 99–103 (2000).

31. F. Tissir, A. Ravni, Y. Achouri, D. Riethmacher, G. Meyer, A. M. Goffinet, DeltaNp73 regulates neuronal survival in vivo. *Proceedings of the National Academy of Sciences* **106**, 16871–16876 (2009).

32. S. N. Schiffmann, B. Bernier, A. M. Goffinet, Reelin mRNA expression during mouse brain development. *Eur. J. Neurosci.* **9**, 1055–1071 (1997).

33. A. Joven, H. Wang, T. Pinheiro, L. S. Hameed, L. Belnoue, A. Simon, Cellular basis of brain maturation and acquisition of complex behaviors in salamanders. *Development* **145**, dev160051 (2018).

34. Z. Yao, C. T. J. van Velthoven, M. Kunst, M. Zhang, D. McMillen, C. Lee, W. Jung, J. Goldy, A. Abdelhak, M. Aitken, K. Baker, P. Baker, E. Barkan, D. Bertagnolli, A. Bhandiwad, C. Bielstein, P. Bishwakarma, J. Campos, D. Carey, T. Casper, A. B. Chakka, R. Chakrabarty, S. Chavan, M. Chen, M. Clark, J. Close, K. Crichton, S. Daniel, P. DiValentin, T. Dolbeare, L. Ellingwood, E. Fiabane, T. Fliss, J. Gee, J. Gerstenberger, A. Glandon, J. Gloe, J. Gould, J. Gray, N. Guilford, J. Guzman, D. Hirschstein, W. Ho, M. Hooper, M. Huang, M. Hupp, K. Jin, M. Kroll, K. Lathia, A. Leon, S. Li, B. Long, Z. Madigan, J. Malloy, J. Malone, Z. Maltzer, N.

Martin, R. McCue, R. McGinty, N. Mei, J. Melchor, E. Meyerdierks, T. Mollenkopf, S. Moonsman, T. N. Nguyen, S. Otto, T. Pham, C. Rimorin, A. Ruiz, R. Sanchez, L. Sawyer, N. Shapovalova, N. Shepard, C. Slaughterbeck, J. Sulc, M. Tieu, A. Torkelson, H. Tung, N. Valera Cuevas, S. Vance, K. Wadhwani, K. Ward, B. Levi, C. Farrell, R. Young, B. Staats, M.-Q. M. Wang, C. L. Thompson, S. Mufti, C. M. Pagan, L. Kruse, N. Dee, S. M. Sunkin, L. Esposito, M. J. Hawrylycz, J. Waters, L. Ng, K. Smith, B. Tasic, X. Zhuang, H. Zeng, A high-resolution transcriptomic and spatial atlas of cell types in the whole mouse brain. *Nature* **624**, 317–332 (2023).

35. Astrid Deryckere, Saket Choudhary, Connor Lynch, Lian Kirit Limperis, Pauline Affatato, Elias Gumnit, Jamie Woych, Alonso Ortega Gurrola, Saeed Tavazoie, Rahul Satija, Christian Mayer, and Maria Antonietta Tosches, A conserved logic for the development of cortical layering in tetrapods.

36. G. La Manno, K. Siletti, A. Furlan, D. Gyllborg, E. Vinsland, A. Mossi Albiach, C. Mattsson Langseth, I. Khven, A. R. Lederer, L. M. Dratva, A. Johnsson, M. Nilsson, P. Lönnerberg, S. Linnarsson, Molecular architecture of the developing mouse brain. *Nature* **596**, 92–96 (2021).

37. M. A. Tosches, T. M. Yamawaki, R. K. Naumann, A. A. Jacobi, G. Tushev, G. Laurent, Evolution of pallium, hippocampus, and cortical cell types revealed by single-cell transcriptomics in reptiles. *Science* **360**, 881–888 (2018).

38. Y. Hao, S. Hao, E. Andersen-Nissen, W. M. Mauck 3rd, S. Zheng, A. Butler, M. J. Lee, A. J. Wilk, C. Darby, M. Zager, P. Hoffman, M. Stoeckius, E. Papalexi, E. P. Mimitou, J. Jain, A. Srivastava, T. Stuart, L. M. Fleming, B. Yeung, A. J. Rogers, J. M. McElrath, C. A. Blish, R. Gottardo, P. Smibert, R. Satija, Integrated analysis of multimodal single-cell data. *Cell* **184**, 3573–3587.e29 (2021).

39. S. Pandey, A. J. Moyer, S. B. Thyme, A single-cell transcriptome atlas of the maturing zebrafish telencephalon. *Genome Res.* **33**, 658–671 (2023).

40. L. Anneser, C. Satou, H.-R. Hotz, R. W. Friedrich, Molecular organization of neuronal cell types and neuromodulatory systems in the zebrafish telencephalon. *Curr. Biol.* **34**, 298–312.e4 (2024).

41. J. Woych, A. Ortega Gurrola, A. Deryckere, E. C. B. Jaeger, E. Gumnit, G. Merello, J. Gu, A. Joven Araus, N. D. Leigh, M. Yun, A. Simon, M. A. Tosches, Cell-type profiling in salamanders identifies innovations in vertebrate forebrain evolution. *Science* **377**, eabp9186 (2022).

42. S. Zeppilli, T. Ackels, R. Attey, N. Klimpert, K. D. Ritola, S. Boeing, A. Crombach, A. T. Schaefer, A. Fleischmann, Molecular characterization of projection neuron subtypes in the mouse olfactory bulb. *Elife* **10**, e65445 (2021).

43. E. S. Lein, M. J. Hawrylycz, N. Ao, M. Ayres, A. Bensinger, A. Bernard, A. F. Boe, M. S. Boguski, K. S. Brockway, E. J. Byrnes, L. Chen, L. Chen, T.-M. Chen, M. C. Chin, J. Chong, B. E. Crook, A. Czaplinska, C. N. Dang, S. Datta, N. R. Dee, A. L. Desaki, T. Desta, E. Diep, T. A. Dolbeare, M. J. Donelan, H.-W. Dong, J. G. Dougherty, B. J. Duncan, A. J. Ebbert, G. Eichele, L. K. Estin, C. Faber, B. A. Facer, R. Fields, S. R. Fischer, T. P. Fliss, C. Frensley, S. N. Gates, K. J. Glattfelder, K. R. Halverson, M. R. Hart, J. G. Hohmann, M. P. Howell, D. P. Jeung, R. A. Johnson, P. T. Karr, R. Kawal, J. M. Kidney, R. H. Knapik, C. L. Kuan, J. H. Lake, A. R.

Laramee, K. D. Larsen, C. Lau, T. A. Lemon, A. J. Liang, Y. Liu, L. T. Luong, J. Michaels, J. J. Morgan, R. J. Morgan, M. T. Mortrud, N. F. Mosqueda, L. L. Ng, R. Ng, G. J. Orta, C. C. Overly, T. H. Pak, S. E. Parry, S. D. Pathak, O. C. Pearson, R. B. Puchalski, Z. L. Riley, H. R. Rockett, S. A. Rowland, J. J. Royall, M. J. Ruiz, N. R. Sarno, K. Schaffnit, N. V. Shapovalova, T. Sivisay, C. R. Slaughterbeck, S. C. Smith, K. A. Smith, B. I. Smith, A. J. Sodt, N. N. Stewart, K.-R. Stumpf, S. M. Sunkin, M. Sutram, A. Tam, C. D. Teemer, C. Thaller, C. L. Thompson, L. R. Varnam, A. Visel, R. M. Whitlock, P. E. Wohnoutka, C. K. Wolkey, V. Y. Wong, M. Wood, M. B. Yaylaoglu, R. C. Young, B. L. Youngstrom, X. F. Yuan, B. Zhang, T. A. Zwingman, A. R. Jones, Genome-wide atlas of gene expression in the adult mouse brain. *Nature* **445**, 168–176 (2007).

44. C. Tufo, S. Poopalasundaram, A. Dorrego-Rivas, M. C. Ford, A. Graham, M. S. Grubb, Development of the mammalian main olfactory bulb. *Development* **149**, dev200210 (2022).

45. E. Winpenny, M. Lebel-Potter, M. E. Fernandez, M. S. Brill, M. Götz, F. Guillemot, O. Raineteau, Sequential generation of olfactory bulb glutamatergic neurons by Neurog2-expressing precursor cells. *Neural Dev.* **6**, 12 (2011).

46. L. Roybon, T. L. Mastracci, J. Li, S. R. W. Stott, A. B. Leiter, L. Sussel, P. Brundin, J.-Y. Li, The Origin, Development and Molecular Diversity of Rodent Olfactory Bulb Glutamatergic Neurons Distinguished by Expression of Transcription Factor NeuroD1. *PLoS One* **10**, e0128035 (2015).

47. B. Zaremba, A. Fallahshahroudi, C. Schneider, J. Schmidt, I. Sarropoulos, E. Leushkin, B. Berki, E. Van Poucke, P. Jensen, R. Senovilla-Ganzo, F. Hervas-Sotomayor, N. Trost, F. Lamanna, M. Sepp, F. García-Moreno, H. Kaessmann, Developmental origins and evolution of pallial cell types and structures in birds. *Science* **387**, eadp5182 (2025).

48. D. Arendt, J. M. Musser, C. V. H. Baker, A. Bergman, C. Cepko, D. H. Erwin, M. Pavlicev, G. Schlosser, S. Widder, M. D. Laubichler, G. P. Wagner, The origin and evolution of cell types. *Nat. Rev. Genet.* **17**, 744–757 (2016).

49. B. Murillo, N. Ruiz-Reig, M. Herrera, A. Fairén, E. Herrera, Zic2 Controls the Migration of Specific Neuronal Populations in the Developing Forebrain. *J. Neurosci.* **35**, 11266–11280 (2015).

50. V. Borrell, O. Marín, Meninges control tangential migration of hem-derived Cajal-Retzius cells via CXCL12/CXCR4 signaling. *Nat. Neurosci.* **9**, 1284–1293 (2006).

51. C. Gil-Sanz, S. J. Franco, I. Martinez-Garay, A. Espinosa, S. Harkins-Perry, U. Müller, Cajal-Retzius cells instruct neuronal migration by coincidence signaling between secreted and contact-dependent guidance cues. *Neuron* **79**, 461–477 (2013).

52. A. Saulnier, M. Keruzore, S. De Clercq, I. Bar, V. Moers, D. Magnani, T. Walcher, C. Filippis, S. Kricha, D. Parlier, L. Viviani, C. K. Matson, Y. Nakagawa, T. Theil, M. Götz, A. Mallamaci, J.-C. Marine, D. Zarkower, E. J. Bellefroid, The doublesex homolog Dmrt5 is required for the development of the caudomedial cerebral cortex in mammals. *Cereb. Cortex* **23**, 2552–2567 (2013).

53. D. Huilgol, S. Udin, T. Shimogori, B. Saha, A. Roy, S. Aizawa, R. F. Hevner, G. Meyer, T. Ohshima, S. J. Pleasure, Y. Zhao, S. Tole, Dual origins of the mammalian accessory olfactory bulb revealed by an evolutionarily conserved migratory stream. *Nat. Neurosci.* **16**, 157–165 (2013).

54. A. Alonso, C. M. Trujillo, L. Puelles, Longitudinal developmental analysis of prethalamic eminence derivatives in the chick by mapping of Tbr1 in situ expression. *Brain Struct. Funct.* **225**, 481–510 (2020).

55. I. Quintana-Urzainqui, P. A. Oel, T. Gerber, L. Pan, N. Papadopoulos, Z. G. Serka, A. Verbanac, M. Börsig, D. Torres-Sabino, I. C. Rollán-Delgado, L. Santangeli, H. Kaessmann, D. Arendt, Developmental landscape of shark telencephalon sheds light on the evolution of telencephalic cell types and the ancient origin of Cajal-Retzius cells, *bioRxiv* (2025)p. 2025.05.08.652169.

56. A. Vílchez-Acosta, Y. Manso, A. Cárdenas, A. Elias-Tersa, M. Martínez-Losa, M. Pascual, M. Álvarez-Dolado, A. C. Nairn, V. Borrell, E. Soriano, Specific contribution of Reelin expressed by Cajal–Retzius cells or GABAergic interneurons to cortical lamination. *Proceedings of the National Academy of Sciences* **119**, e2120079119 (2022).

57. M. Anstötz, S. K. Lee, G. Maccaferri, Glutamate released by Cajal-Retzius cells impacts specific hippocampal circuits and behaviors. *Cell Rep.* **39**, 110822 (2022).

58. M. Riva, S. Moriceau, A. Morabito, E. Dossi, C. Sanchez-Bellot, P. Azzam, A. Navas-Olive, B. Gal, F. Dori, E. Cid, F. Ledonne, S. David, F. Trovero, M. Bartolomucci, E. Coppola, N. Rebola, A. Depaulis, N. Rouach, L. M. de la Prida, F. Oury, A. Pierani, Aberrant survival of hippocampal Cajal-Retzius cells leads to memory deficits, gamma rhythmopathies and susceptibility to seizures in adult mice. *Nat. Commun.* **14**, 1531 (2023).

59. Y. Choe, J. A. Siegenthaler, S. J. Pleasure, A cascade of morphogenic signaling initiated by the meninges controls corpus callosum formation. *Neuron* **73**, 698–712 (2012).

60. A. Aguiló, T. H. Schwartz, V. S. Kumar, Z. A. Peterlin, A. Tsiola, E. Soriano, R. Yuste, Involvement of cajal-retzius neurons in spontaneous correlated activity of embryonic and postnatal layer 1 from wild-type and reeler mice. *J. Neurosci.* **19**, 10856–10868 (1999).

61. J. Fournier, C. M. Müller, G. Laurent, Looking for the roots of cortical sensory computation in three-layered cortices. *Curr. Opin. Neurobiol.* **31**, 119–126 (2015).

62. A. Damilou, L. Cai, A. Ö. Argunşah, S. Han, G. Kanatouris, M. Karatsoli, O. Hanley, L. Gesuita, S. Kollmorgen, F. Helmchen, T. Karayannis, Developmental Cajal-Retzius cell death contributes to the maturation of layer 1 cortical inhibition and somatosensory processing. *Nat. Commun.* **15**, 6501 (2024).

63. G. F. Striedter, R. G. Northcutt, The independent evolution of dorsal pallia in multiple vertebrate lineages. *Brain Behav. Evol.* **96**, 200–211 (2022).

64. A. Hayar, M. T. Shipley, M. Ennis, Olfactory bulb external tufted cells are synchronized by multiple intraglomerular mechanisms. *J. Neurosci.* **25**, 8197–8208 (2005).

65. R. Tatti, K. Bhaukaurally, O. Gschwend, R. P. Seal, R. H. Edwards, I. Rodriguez, A. Carleton, A population of glomerular glutamatergic neurons controls sensory information transfer in the mouse olfactory bulb. *Nat. Commun.* **5**, 3791 (2014).

66. M. Antal, M. Eyre, B. Finklea, Z. Nusser, External tufted cells in the main olfactory bulb form two distinct subpopulations. *Eur. J. Neurosci.* **24**, 1124–1136 (2006).

67. G. Quattrocolo, G. Maccaferri, Novel GABAergic circuits mediating excitation/inhibition of Cajal-Retzius cells in the developing hippocampus. *J. Neurosci.* **33**, 5486–5498 (2013).

68. A. Hayar, S. Karnup, M. Ennis, M. T. Shipley, External tufted cells: a major excitatory element that coordinates glomerular activity. *J. Neurosci.* **24**, 6676–6685 (2004).

69. T. Hirata, T. Kumada, T. Kawasaki, T. Furukawa, A. Aiba, F. Conquet, Y. Saga, A. Fukuda, Guidepost neurons for the lateral olfactory tract: expression of metabotropic glutamate receptor 1 and innervation by glutamatergic olfactory bulb axons. *Dev. Neurobiol.* **72**, 1559–1576 (2012).

70. Z. Molnár, H. J. Luhmann, P. O. Kanold, Transient cortical circuits match spontaneous and sensory-driven activity during development. *Science* **370**, eabb2153 (2020).

71. D. Arendt, The evolution of cell types in animals: emerging principles from molecular studies. *Nat. Rev. Genet.* **9**, 868–882 (2008).

72. M. Puopolo, O. Belluzzi, Inhibitory synapses among interneurons in the glomerular layer of rat and frog olfactory bulbs. *J. Neurophysiol.* **80**, 344–349 (1998).

73. M. Marín-Padilla, Three-dimensional structural organization of layer I of the human cerebral cortex: a Golgi study: LAYER I OF HUMAN CEREBRAL CORTEX. *J. Comp. Neurol.* **299**, 89–105 (1990).

74. D. M. Gallien L, Table chronologique du développement chez Pleurodeles Waltlii Michah. *Bull. Bio* (1957).

75. V. Hamburger, H. L. Hamilton, A series of normal stages in the development of the chick embryo. 1951. *Dev. Dyn.* **195**, 231–272 (1992).

76. J. A. Gillis, S. Bennett, K. E. Criswell, J. Rees, V. A. Sleight, C. Hirschberger, D. Calzarette, S. Kerr, J. Dasen, Big insight from the little skate: Leucoraja erinacea as a developmental model system. *Curr. Top. Dev. Biol.* **147**, 595–630 (2022).

77. M. Andreatta, S. J. Carmona, UCell: Robust and scalable single-cell gene signature scoring. *Comput. Struct. Biotechnol. J.* **19**, 3796–3798 (2021).

78. F. Svara, D. Förster, F. Kubo, M. Januszewski, M. Dal Maschio, P. J. Schubert, J. Kornfeld, A. A. Wanner, E. Laurell, W. Denk, H. Baier, Automated synapse-level reconstruction of neural circuits in the larval zebrafish brain. *Nat. Methods* **19**, 1357–1366 (2022).

79. C. P. Cantalapiedra, A. Hernández-Plaza, I. Letunic, P. Bork, J. Huerta-Cepas, EggNOG-mapper v2: Functional annotation, orthology assignments, and domain prediction at the metagenomic scale. *Mol. Biol. Evol.* **38**, 5825–5829 (2021).

80. H. M. T. Choi, M. Schwarzkopf, M. E. Fornace, A. Acharya, G. Artavanis, J. Stegmaier, A. Cunha, N. A. Pierce, Third-generation in situ hybridization chain reaction: multiplexed, quantitative, sensitive, versatile, robust. *Development* **145**, dev165753 (2018).

81. E. C. B. Jaeger, D. Vijatovic, A. Deryckere, N. Zorin, A. L. Nguyen, G. Ivanian, J. Woych, R. C. Arnold, A. O. Gurrola, A. Shvartsman, F. Barbieri, F. A. Toma, H. T. Cline, T. F. Shay, D. B. Kelley, A. Yamaguchi, M. Shein-Idelson, M. A. Tosches, L. B. Sweeney, Adeno-associated viral tools to trace neural development and connectivity across amphibians. *Dev. Cell* **60**, 794–812.e6 (2025).

82. E. Kuehn, D. S. Clausen, R. W. Null, B. M. Metzger, A. D. Willis, B. D. Özpolat, Segment number threshold determines juvenile onset of germline cluster expansion in Platynereis dumerilii. *J. Exp. Zool. B Mol. Dev. Evol.* **338**, 225–240 (2022).

83. M. F. Wullimann, N. Mokayes, I. Shainer, E. Kuehn, H. Baier, Genoarchitectonics of the larval zebrafish diencephalon. *J. Comp. Neurol.* **532**, e25549 (2024).

84. M. Kunst, E. Laurell, N. Mokayes, A. Kramer, F. Kubo, A. M. Fernandes, D. Förster, M. Dal Maschio, H. Baier, A cellular-resolution atlas of the larval zebrafish brain. *Neuron* **103**, 21–38.e5 (2019).

85. J. W. Kenney, P. E. Steadman, O. Young, M. T. Shi, M. Polanco, S. Dubaishi, K. Covert, T. Mueller, P. W. Frankland, A 3D adult zebrafish brain atlas (AZBA) for the digital age. *Elife* **10** (2021).

**Acknowledgments:** we thank Nandan Nerurkar and Elanur Yilmaz (Columbia University) for providing chick and zebrafish samples, the Columbia ICM team for excellent animal care, and Tosches lab members for feedback throughout the project. Light-sheet imaging was performed with support from the Zuckerman Institute's Cellular Imaging platform (NIH grant 1S10OD023587-01). Computing resources were provided by Columbia University's Shared Research Computing Facility (NIH grant 1G20RR030893-01 and NYSTAR contract C090171).

**Funding:**

National Institute of Health NIGMS R35GM146973

National Institute of Health NHGRI RM1HG011014

the Rita Allen Foundation

the Chan Zuckerberg Initiative (M.A.T.)

the National Science Foundation (Graduate Research Fellowship to E.G.)

the Revson Foundation (G.G.)

an EMBO Long-Term Fellowship (A.D.)

the Karen Toffler Charitable Trust Scholar Program (P.B.)

the Thompson Family Foundation Program for Accelerated Medicine Exploration in Alzheimer's Disease and Related Disorders of the Nervous System (TAME-AD) (C.K.).
**Author contributions:** M.A.T. acquired funding and supervised the study. E.G., G.G., A.D, M.A.T. analyzed scRNA-seq data, and E.G. performed cross-species comparisons. E.G., G.G., P. B., J A.G., C.K. and J.W. prepared samples for histology. E.G., G.G., and J.W., performed histology and imaging. E.G. and M.A.T. wrote the manuscript, with edits from G.G., J.W., A.D., and C.K.

**Supplementary Materials**

Materials and Methods

Figs. S1 to S13

References (*71-85*)

Movies S1 to S4

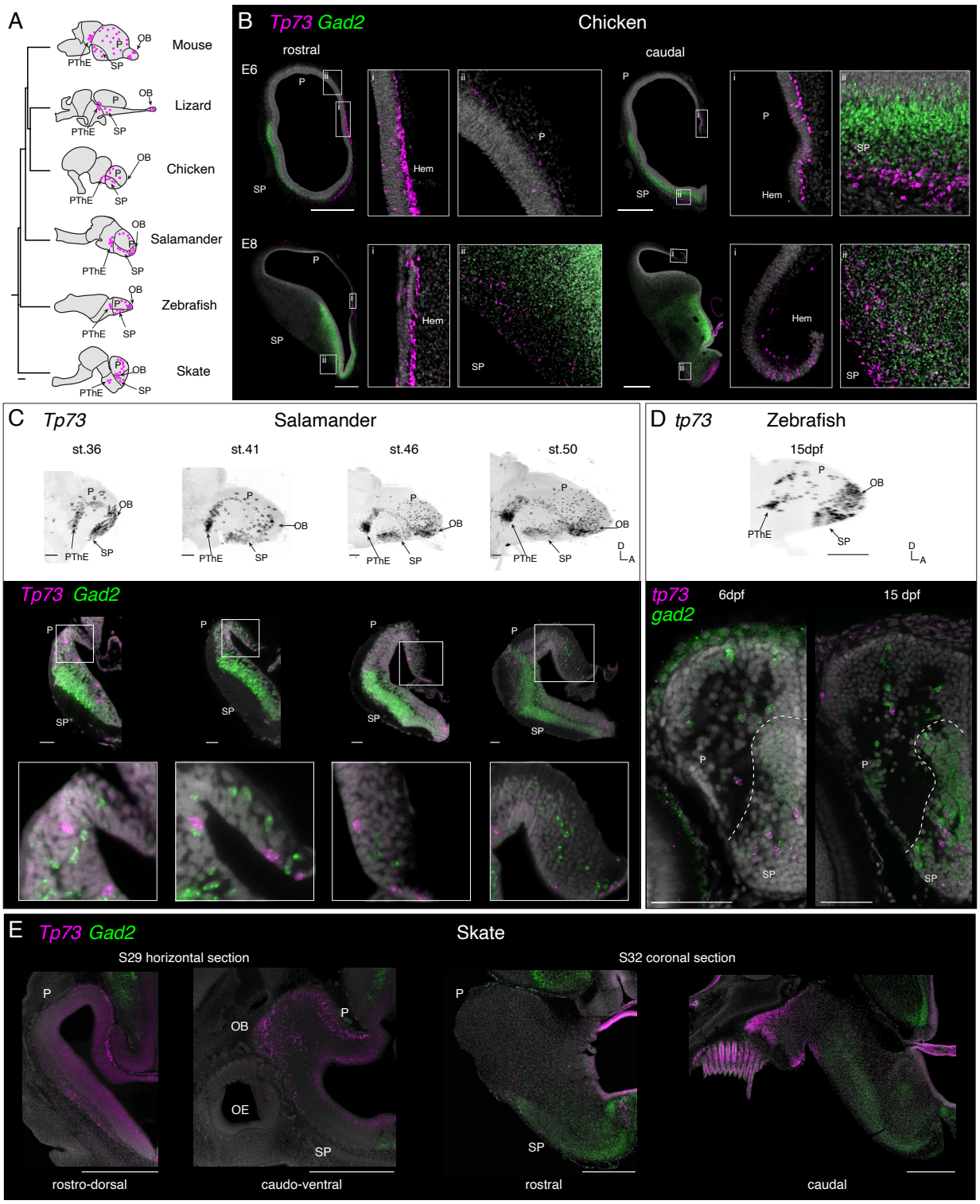


**Fig. 1. Conserved *Tp73* expression in vertebrate forebrains.**
(**A**) Distribution of *Tp73* neurons in vertebrate brains, according to published data and this study. Scale bar: 100 million years. (**B**) Double HCRs for *Tp73* (magenta) and *Gad2* (green) in coronal sections of chick brains (embryonic stages E6 and E8), showing *Tp73* expression in the developing hem, pallium, and subpallium. *Gad2* labels GABAergic neurons and helps identify the pallial-subpallial boundary. Scale bars = 500 um. (**C**) Top: 3D max intensity projections (lateral views, anterior on the right) of salamander brains (larval stages 36, 41, 46, and 50) after

whole mount HCR for *Tp73.* Scale bar 100um. Bottom: optical coronal sections through one telencephalic hemisphere of *Tp73* and *Gad2*-labeled brains at different developmental stages; insets show *Tp73*+ and *Gad2*+ neurons in pallium. Scale bar 50 um. (**D**) 3D max intensity projection of a whole mount 15 dpf zebrafish brain (lateral view, anterior on the right) after HCR for *tp73.* Scale bar 100 um. Bottom: sections of *tp73* and *gad2*-labeled 6 dpf and 15dpf zebrafish brains showing *tp73*+ and *gad2*+ neurons in pallium and subpallium. Scale bar 50 um. (**E**) Expression of *Tp73* and *Gad2* in the developing skate brain. Left: horizontal sections of stage 29 brains; right: coronal sections of stage 32 brains. Scale bar 500um. See additional sections in fig. S1.

Abbreviations: E, embryonic day; P, pallium; SP, subpallium; OB, olfactory bulb; OE, olfactory epithelium; PThE, prethalamic eminence; dpf, days post fertilization; A, anterior; D, dorsal.

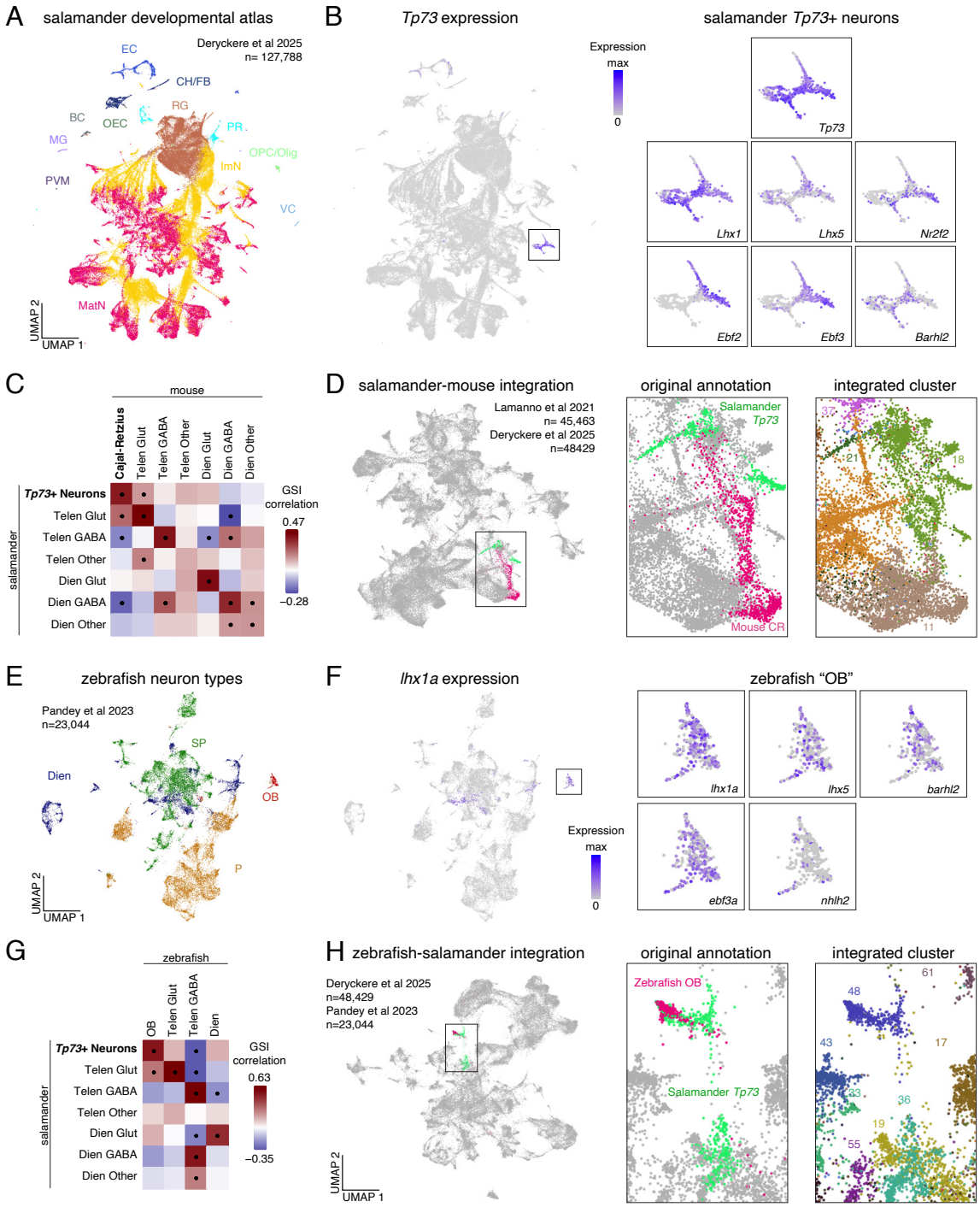


**Fig. 2. Mouse, salamander, and zebrafish *Tp73*+ neurons have a shared transcriptomic signature.**

(**A**) UMAP of the Deryckere et al. (*35*) scRNA-seq dataset from the developing salamander brain (n=127,788 cells), showing cells colored by broad class. (**B**) Left: UMAP showing *Tp73* expression in the developing salamander brain dataset. Right: Zoom on *Tp73*+ neurons, showing the expression of known CR marker TFs (*5*) (fig. S3A for full UMAPs of zoomed genes). (**C**) Pairwise GSI correlations of classes of salamander and mouse forebrain neurons (mouse data from (*36*)). Correlations based on the intersection of genes that were differentially expressed in both mouse and salamander (344 total genes). Dots indicate statistically significant correlations.

(**D**) UMAP showing forebrain neurons from developing salamander and mouse after Seurat CCA integration. Salamander *Tp73*+ neurons and mouse CR cells highlighted in green and magenta, respectively. Right: Zoom on integrated cluster 18 containing salamander *Tp73* neurons and mouse CR cells. (**E**) UMAP of the Pandey et al 2023 (*39*) dataset from the developing zebrafish telencephalon (n=23,044 cells, stages 6 and 15 dpf only), showing cells colored by type. (**F**) Left: UMAP showing *lhx1a* expression in the larval zebrafish dataset. Right: Zoom on zebrafish OB neurons showing expression of *lhx1a* and other CR TFs. (**G**) Pairwise GSI correlations of classes of salamander and zebrafish forebrain neurons. Correlations based on the intersection of genes that were differentially expressed in both zebrafish and salamander (149 total genes). Dots indicate statistically significant correlations. (**H**) UMAP showing forebrain neurons from developing salamander and zebrafish after Seurat CCA integration. Right: Zoom on integrated cluster 48 containing salamander *Tp73* neurons and zebrafish OB cells.

Abbreviations: BC, blood cells; CH/FB, chondrocytes/fibroblasts; EC, epithelial cells; Dien, diencephalon; GABA, GABAergic; Glut, glutamatergic; GSI, gene specificity index; ImN, immature neurons; MatN, mature neurons; MG, microglia; OEC, olfactory ensheathing cells; OPC/Olig, oligodendrocyte precursor cells/oligodendrocytes; P, pallium; PVM, perivascular macrophages; PR, photoreceptor cells; RG, radial glia; SP, subpallium; Telen, telencephalon; VC, vascular cells; see also Fig. 1.

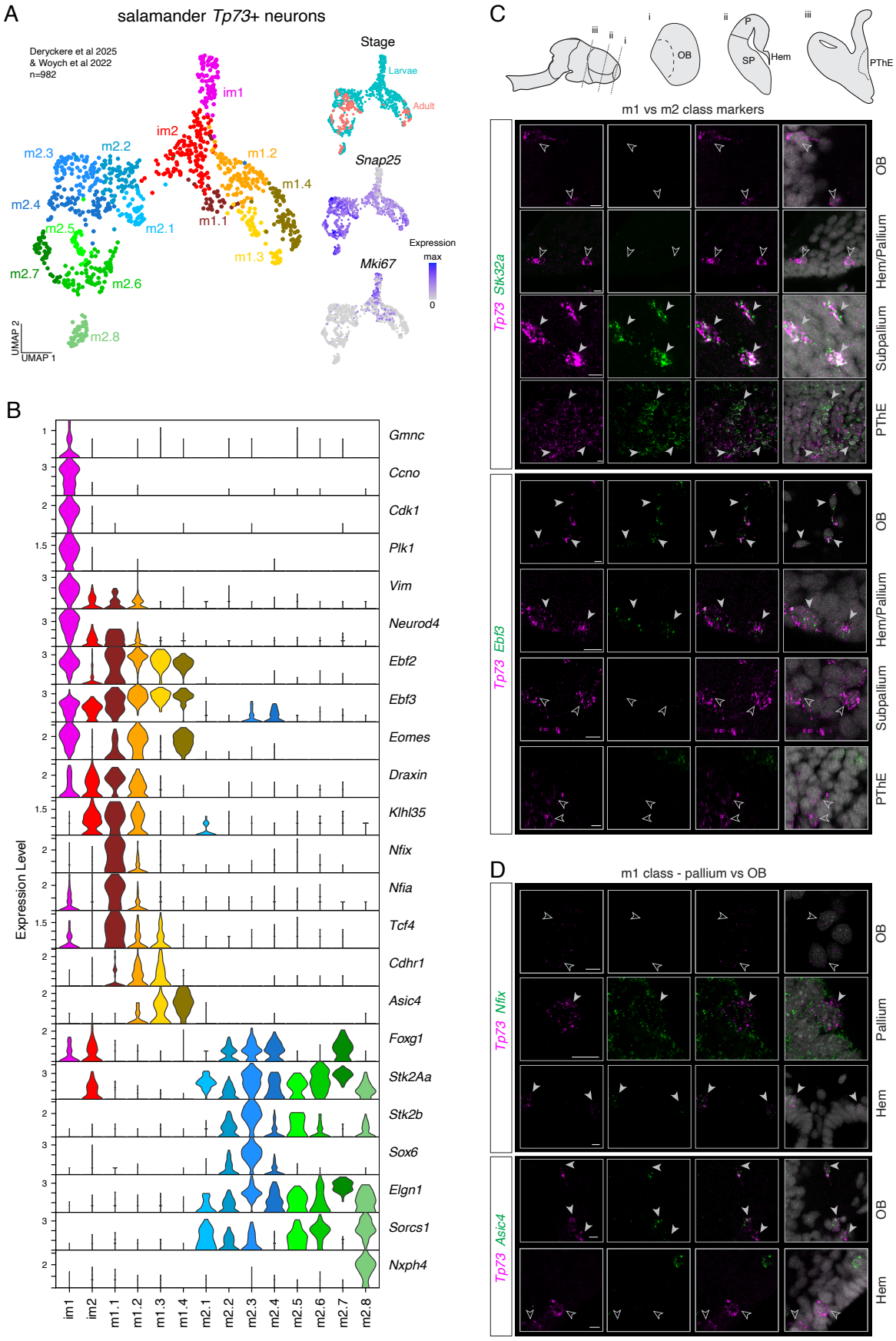
A
salamander Tp73+ neurons
Deryckere et al 2025
& Woych et al 2022
n=982
Stage
Larvae
Adult
Snap25
Mki67
Expression
max
0
im1
im2
m1.1
m1.2
m1.3
m1.4
m2.1
m2.2
m2.3
m2.4
m2.5
m2.6
m2.7
m2.8
UMAP 2
UMAP 1
B
Expression Level
Gmnc
Ccno
Cdk1
Plk1
Vim
Neurod4
Ebf2
Ebf3
Eomes
Draxin
Klhl35
Nfix
Nfia
Tcf4
Cdhr1
Asic4
Foxg1
Stk2Aa
Stk2b
Sox6
Elgn1
Sorcs1
Nxph4
C
OB
SP
P
Hem
PThE
m1 vs m2 class markers
Tp73 Stk32a
Tp73 Ebf3
Hem/Pallium
Subpallium
D
m1 class - pallium vs OB
Tp73 Nfix
Tp73 Asic4
Pallium

**Fig. 3. Transcriptomic and spatial heterogeneity of salamander *Tp73*+ neurons**
(**A**) UMAPs of the salamander *Tp73*+ neurons dataset (n= 982 cells). Left: *Tp73*+ neurons colored by cluster. Right: *Tp73*+ neurons colored by dataset (adult from (*41*)), and expression of *Snap25* and *Mki67*. (**B**) Violin plots showing the expression of marker genes for *Tp73* neuronal clusters; m1 and m2 populations express different sets of markers. (**C**)-(**D**) Closeups showing coexpression of *Tp73* and selected marker genes detected by HCR in late active larvae (stages 46-55; see fig S8 for full images). (C) Top: coexpression of *Stk32a* and *Tp73* in PthE and subpallium but not in OB and hem/pallium. Bottom: *Ebf3* and *Tp73* coexpression in OB and hem/pallium but not subpallium and PThEregions. Scale bar 10um. (D) Top: coexpression of *Nfix* and *Tp73* in pallium but not OB. Bottom: coexpression of *Asic4* and *Tp73* in OB but not hem. Scale bar: 10 um.

Abbreviations: im, immature; m, mature; see also Figure 1.

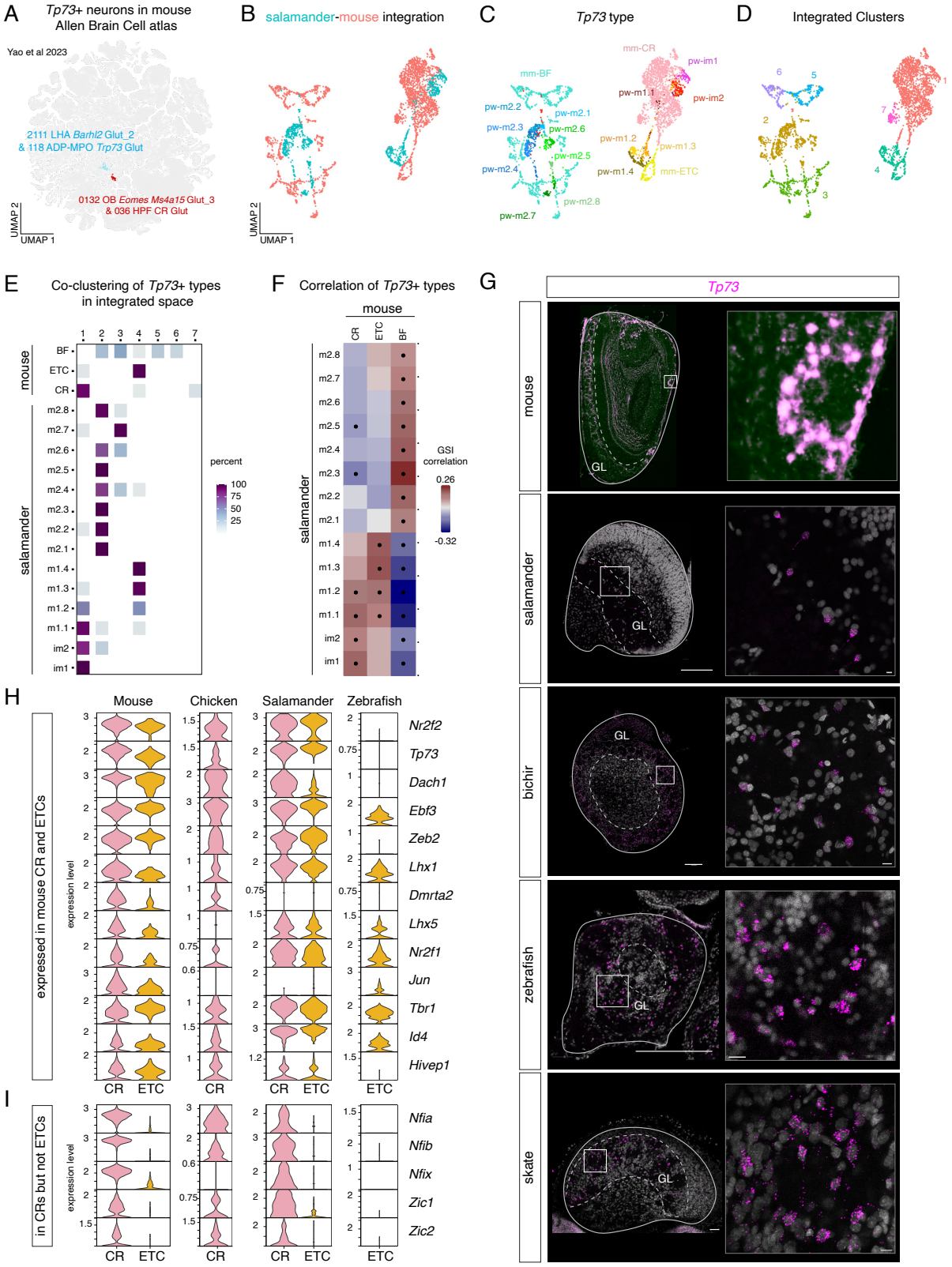


**Fig. 4. Transcriptomic similarity of CR and *Tp73*+ external tufted cells in mouse and salamander.**

(**A**) UMAP of the mouse Allen Brain Cell atlas (*34*), highlighting the *Tp73*+ cells used for further analysis. (**B-D**) UMAPs showing salamander and mouse *Tp73*+ neurons after Seurat CCA integration, with cells colored by species (B), original neuron type annotation (**C**), and integrated cluster (**D**). (**E**) Matrix showing the percentage of cells of each *Tp73* type (original annotations, rows) included the new integrated clusters (columns). (**F**) Pairwise GSI correlations of mouse and salamander *Tp73*+ types. Correlations based on the intersection of genes differentially expressed in both mouse and salamander (647 total). Dots indicate statistically significant correlations. (**G**).*Tp73*+ neurons in the OB glomerular layer of mouse (adult), salamander (adult), bichir fish (adult), zebrafish (3 mpf), and skate (adult). Mouse *Trp73* colorimetric *in situ* hybridization adapted from mouse Allen Mouse Brain Atlas, mouse.brain-map.org and atlas.brain-map.org (*43*). All other images are *Tp73* HCRs. Full image scale bars 200um. Zoom scale bars 10um. (**H**) Violin plots showing expression of TFs expressed in mouse CR cells and ETC but not in an outgroup (OB mitral/tufted cells), and the expression of the same TFs in other vertebrate species. (**I**) Violin plots showing expression of TFs expressed in CR cells but not in ETCs in both mouse and salamander, and the expression of the same TFs in chick and zebrafish. Data from (*34*, *35*, *39*, *41*, *47*) (see Methods for details).

Abbreviations: BF, basal forebrain; ETC, external tufted cells; GL, glomerular layer; see also Figures 1, 2, and 3.

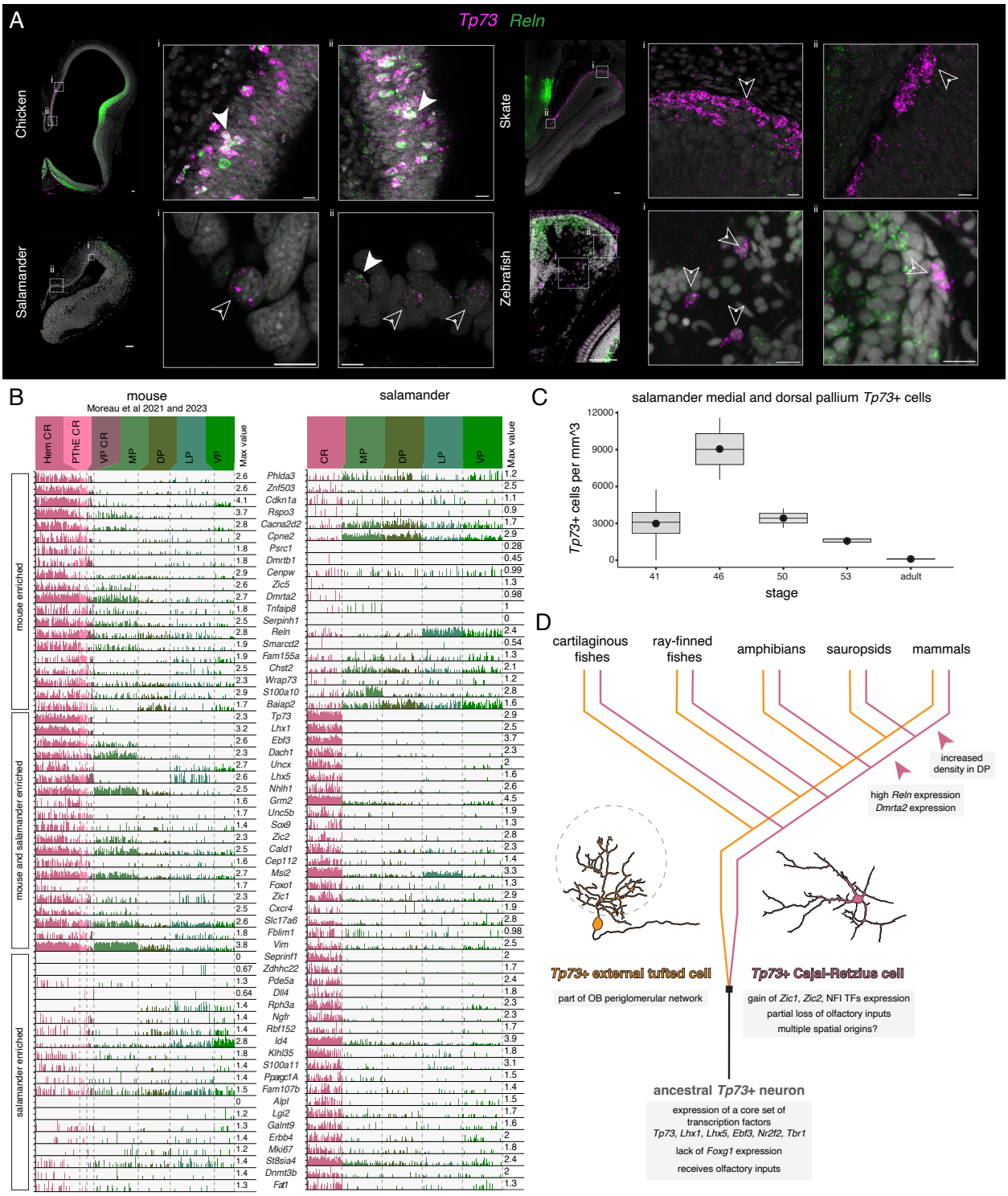


**Fig. 5. Transcriptomic divergence of vertebrate CR cells.**
(**A**) HCRs showing *Reln* (green) and *Tp73* (magenta) expression on coronal sections of developing stage E6 chick, st.50 salamander and 6 dpf zebrafish brains, and an horizontal section of a stage 29 skate brain. Closed arrowheads indicate examples of *Tp73*+ *Reln*+ cells. Open arrowheads indicate examples of *Tp73*+ *Reln*-negative cells. Scale bar 50um (Coronal Section) 10 um (Zoom Panel). (**B**) Expression of marker genes that differentiate CR cells from other pallial glutamatergic neurons (ETCs excluded) in mouse and salamander developmental datasets.

The plot shows the top 20 genes enriched in mouse but not salamander CR cells; the top 20 genes enriched in both species, and the top 20 enriched in salamander but not mouse CR cells (see Methods). Mouse data from Moreau et al 2021 and Moreau et al 2023 (*25*, *29*). (**C**) Quantification of the density of *Tp73+* cells in salamander medial and dorsal pallium across developmental stages. Black dot represents average value. n= 3 animals for stages 36-50 and adult, n=2 for stage 53. (**D**) Proposed evolutionary relationship between CR cells and ETCs. Vertebrate phylogenetic tree with cell type typogenetic tree superimposed (inspired by(*71*)). Schematics of ETC and CR cells (dorsal view) based on(*72*, *73*). Dotted circle represents OB glomerulus.
Abbreviations: DP, dorsal pallium; LP, lateral pallium; MP, medial pallium; VP, ventral pallium